Interaction of polymethacrylate-*g*-PEO comb copolymers with natural bentonite in aqueous systems

Weishan Wang[1], *Baicun Zheng*[1], *Weiguang Gong*[1], *Lefeng Fu*[2], *Zhongjun Feng*[2]

[1]*Research & Development Center for Sports Materials, East China University of Science and Technology, Shanghai 200237, People's Republic of China*
[2]*Shanghai Sunrise Polymer Company Limited, Shanghai 200232, People's Republic of China*
E-mail: wangweishan332@163.com

Published in Micro & Nano Letters; Received on 8th April 2012

Natural bentonite was successfully modified using polymethacrylate-*g*-polyethylene oxide (PEO) comb copolymer. Changes in the surfaces and microstructure of the resultant organo-bentonite were characterised by Fourier transform infrared (FTIR), X-ray diffraction (XRD), thermogravimetric analysis (TG), scanning electron microscopy and high-resolution transmission electron microscopy, respectively. FTIR results indicated the presence of the copolymer on the surface of organo-bentonite. XRD measurements showed that the copolymer molecules were intercalated into the bentonite layers. TG analysis and electron microscopy micrographs demonstrated the interlayers of bentonite were intercalated by the copolymers with surface adsorption to a certain extent.

1. Introduction: Bentonite is a 2:1 type of clay material primarily composed of montmorillonite (smectite group). It is built of packets of two silica tetrahedral sheets sandwiching one aluminum octahedral sheet. As the result of isomorphous substitution of the layers by cations of lower valence (e.g. Al^{3+} replaced by Mg^{2+} or Fe^{2+} in the octahedral sheet; Si^{4+} replaced by Al^{3+} in the tetrahedral sheet), excessive net negative charges appear on the surface of layer lattice. These negative charges are compensated by the adsorption of cations (Na^{+}, Ca^{2+} etc.) in the interlayers. Owing to its excellent physical and chemical characteristics (large specific area, high cation exchange capacity (CEC) and consequential strong adsorption capability), bentonite finds a wide range of applications, such as drilling muds [1, 2], catalysis [3], nanocomposites [4, 5], pollution control [6] and drugs [7].

However, natural bentonite without any modification has narrow layer spacing and strong hydrophilicity [8] caused by the hydration of inorganic cations in the interlayer exchange sites, which limits its further application. For this reason, it is promising to modify natural bentonite to organo-bentonite. The modification of bentonite is always realised by ion exchange of the interlayer inorganic cations with organic surfactants. In hitherto studies, the bentonite interlayer space was filled with amines [9], amino acids [10, 11], cationic surfactants [12–14], non-ionic surfactants [15] etc. The modification treatment not only renders the surface less hydrophilic and hence more hydrophobic but also greatly increases the basal spacing of the layers, which makes bentonite become a more promising material in environmental control [16–18], nanocomposites [19, 20] etc. All of these applications mentioned above depend considerably on the structure and properties of the modified organo-bentonite. Moreover, previous studies [21, 22] show that there exists strong adsorption between clay and organic molecules including superplasticiser, but the interaction mechanism has not been understood thoroughly. For these reasons, research on the interaction between natural bentonite and organic surfactant is of vital theoretical and practical importance.

This research was undertaken to investigate the structural changes of bentonite modified with polymethacrylate-*g*-polyethylene oxide (PEO) comb copolymers – one kind of polycarboxylate-based superplasticiser widely used in mortar and concrete industry [23–25]. Fourier transform infrared (FTIR) analysis was conducted to identify the functional groups in natural and modified bentonite, and provide evidence for modification achieved through the copolymer treatment. Thermogravimetric analysis (TG) was used to evaluate thermal stability and chemical structure of the modified bentonite. X-ray diffraction (XRD) was used to study the intercalation of bentonite modified with the copolymer. The morphology and microstructure of the organo-bentonite were studied using scanning electron microscopy (SEM) and high-resolution transmission electron microscopy (HRTEM), which have been proven to be most useful methods for evaluating the modification of clay surfaces [26, 27].

2. Experimental

2.1. Materials: Natural bentonite was kindly supplied by Huangshan Baiyue Activated Clay Co., Ltd. It was crushed, ground, sieved through a 200 mesh sieve and dried at 105°C in an oven for 2 h prior to use. Chemical analysis of bentonite was performed by sequential X-ray fluorescence spectrometer (XRF-1 800; Shimadzu Corporation) and the results are shown in Table 1. The mineralogical composition of the natural bentonite sample was determined by X-ray diffractograms (shown in Fig. 1). X-ray analysis of the sample was made using the three principal lines [28]. The following mineral phases were identified: montmorillonite, quartz, mica, magnesite, feldspar and calcite. The specific surface area of natural bentonite was found to be 38.6 m^2/g by Brunauer-Emmett-Teller (BET) method using nitrogen as an adsorbent (ASAP 2010N; Macromeritics).

A commercial polycarboxylate-based superplasticiser-labelled PCE-1 (Shanghai Sunrise Polymer Co., Ltd) was selected as the modifier without further purification, which are comb-like copolymers based from a sodium polymethacrylate backbone and grafted side chains of polyethylene oxides (see Fig. 2). All other chemicals were of analytical grade.

2.2. Preparation of the organo-bentonite: Six grams of bentonite was dispersed in 300 mL of deionised water followed by mixing for 1 h at 30°C to swell it. The copolymers were dissolved in 300 mL of deionised water at 30°C (20 g/L) and slowly added to the bentonite suspension. The dispersion was stirred at 30°C for 1 h and filtered using sintered disc filter funnel. The modified bentonite was washed several times with deionised water until free of copolymer in the filtrate detected by UV–vis spectrophotometer (UV-1800; Shanghai Mapada Instruments Co., Ltd.). The complex was resuspended in deionised water and centrifuged. The obtained organo-bentonite was dried at 80°C in a hot air oven, and then gently crushed, ground in an agate mortar to pass through a 200 mesh sieve and kept in a sealed bottle for further characterisation.

Table 1 Main chemical composition of bentonite

Chemical composition, wt%									LOI, wt%
SiO_2	Al_2O_3	MgO	CaO	Fe_2O_3	TiO_2	K_2O	Na_2O	P_2O_5	
72.99	16.33	4.67	3.18	1.78	0.35	0.17	0.04	0.05	11.70

LOI, loss of ignition at 1000°C.

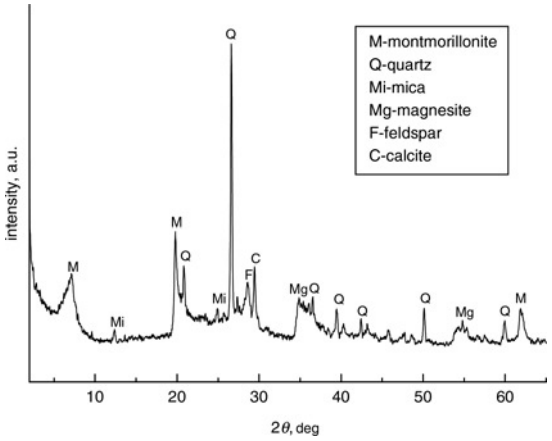

Figure 1 *XRD pattern of natural bentonite*

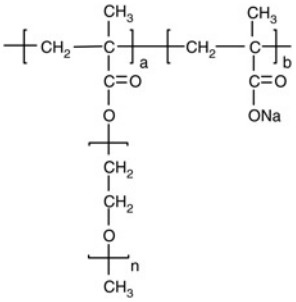

Figure 2 *Chemical structure of the copolymer*

2.3. Characterisation methods: FTIR spectra of samples were acquired by a 6700 FTIR spectrometer (Nicolet) using KBr pressed disk technique. Natural bentonite and KBr were weighted and then were ground in an agate mortar prior to pellet making. The spectra were obtained by accumulating 32 scans at a resolution of 2 cm^{-1} in the range of 4000–400 cm^{-1}.

TG and differential thermogravimetric (DTG) curves were obtained simultaneously by using a STD Q600 thermal analyser (TA). The measurements were conducted in high-purity flowing nitrogen atmosphere (100 mL/min) and the test temperature was from 25 to 800°C with a heating rate of 20°C/min. Approximately 20 mg sample was heated in an oven alumina crucible.

The X-ray studies were performed using the powder diffraction technique. The analysis was conducted using a D/MAX 2550 VB/PC diffractometer (Rigaku). The source of X-ray radiation was a sealed tube with a copper anode and nickel filter supplied by the generator (40 kV, 100 mA). Diffraction measurements were conducted with the 2θ angle of 2–80° at the scanning rate of 0.02°/min. The basal spacing was calculated by using Bragg's equation (1)

$$n\lambda = 2d \sin\theta \quad (1)$$

where n is the integer ($n = 1$), λ is the wavelength of incident wave ($\lambda = 0.15418$ nm), d is the spacing between the layers in the bentonite lattice and θ is the angle between the incident ray and the scattering planes.

A JSM-6360LV SEM (JEOL) was used for the morphological studies. The bentonite and organo-bentonite samples were dried at 80°C and coated with gold under vacuum conditions in an argon atmosphere ionisation chamber for the following test. JEM-2100 high-resolution TEM (JEOL) was used to investigate the microstructure of natural and organo-bentonite at an accelerating voltage of 200 kV. Bentonite samples were dispersed in ethanol ultrasonically for 30 min and dropped on Cu mesh grids coated carbon, then dried in an hot air oven at 50°C for 10 min.

3. Results and discussion

3.1. FTIR spectra: FTIR is a sensitive method to probe the molecular environment of organic groups with the organoclay [29]. The FTIR spectra of bentonite and organo-bentonite are shown in Fig. 3, depicting the major changes of bentonite before and after the modification with the copolymer. After the modification of polymethacrylate-*g*-PEO copolymer, the spectra of the organo-bentonite not only had characteristic bentonite bands, but also exhibited some new characteristic bands.

As can be seen from Fig. 3, the adsorption peak at 3620 cm^{-1} was assigned to the –OH stretching vibration of water molecules within the bentonite interlayer and weakly bonded to the Si–O surface, and the broad peak centred at 3470 cm^{-1} was due to the –OH stretching vibration of adsorbed water. The peak at around 1640 cm^{-1} corresponded to the –OH deformation of water in both natural bentonite and organo-bentonite, but the peak intensity of organo-bentonite was lower than natural bentonite. This might be acceptable evidence for the increased hydrophobicity of the bentonite surface because of the copolymer modification. The bands observed at ~1110 and 1040 cm^{-1} represented the Si–O coordination vibrations and the stretching vibrations of Si–O in the Si–O–Si groups of the tetrahedral sheet, respectively, which corresponded to the characteristic band of montmorillonite [30]. The –OH bending vibration peaks of octahedral layer was observed at 914 cm^{-1} (AlAlOH) and 847 cm^{-1} (AlMgOH), which pointed

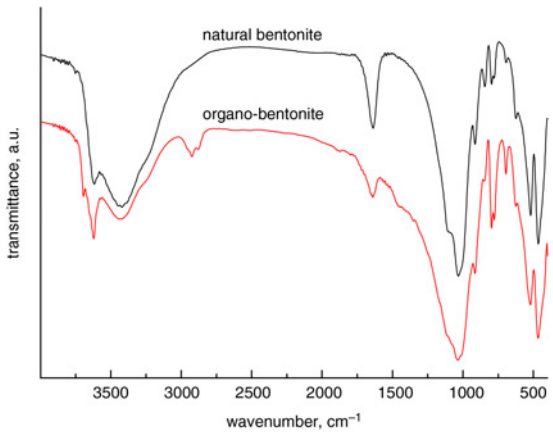

Figure 3 *FTIR spectra of natural and organo-bentonite*

doi: 10.1049/mnl.2012.0251

out the octahedral substitution process. The peaks originating from the external bentonite components (e.g. quartz) were located at 796, 779 and 694 cm^{-1}. Also, 625, 521 and 467 cm^{-1} were assigned to the Si–O stretching vibration, Si–O–Al (octahedral) bending vibration and Si–O–Si bending vibration, respectively.

Compared to natural bentonite, the spectra of organo-bentonite showed two additional peaks at 2923 and 2879 cm^{-1}, which were attributed to the asymmetric and symmetric stretching vibrations of the methyl and methylene groups. This observation also indicated the presence of the polymethacrylate-*g*-PEO copolymer on the surface of organo-bentonite.

3.2. X-ray diffraction: The most widely used method for the study of intercalation surfactants in the galleries of phyllosilicates is XRD, which provides information on the interlayer structure of surfactant [31]. The XRD patterns of natural bentonite and organo-bentonite modified by the polymethacrylate-*g*-PEO copolymer are shown in Fig. 4. An intense reflection at $2\theta = 7.14^{o}$ (corresponding interlayer distance was 1.24 nm) was observed for natural bentonite, which was attributed to the d_{001} plane of montmorillonite. In comparison with natural bentonite, the d_{001} peak of organo-bentonite shifted towards lower angle 6.18°, responding to a basal spacing of 1.43 nm, indicating the expansion of the interlayer space because of the intercalation of the copolymer molecules.

3.3. TG analysis: The TG and DTG curves of natural bentonite (see Fig. 5) showed two main stages of mass losses. In the first stage, the evolution of physically adsorbed water on the surface of natural bentonite in the region of 22–175°C gave rise to a peak

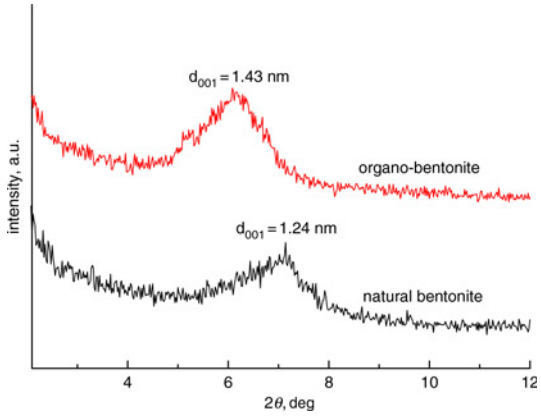

Figure 4 *XRD patterns of natural bentonite and organo-bentonite*

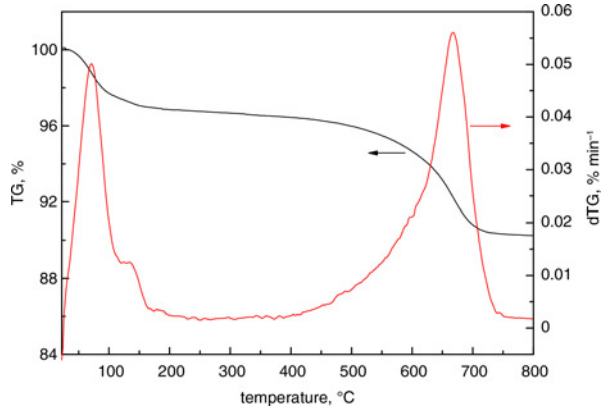

Figure 5 *TG/DTG curves of natural bentonite*

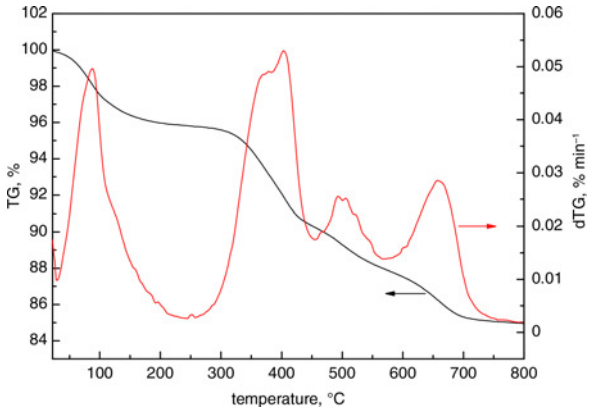

Figure 6 *TG/DTG curves of organo-bentonite*

maximum of 71°C on the DTG curve. The peak at 134°C which was accompanied by a mass loss of 0.30%, was ascribed to the elimination of the water species coordinated to the interlayer cations. In addition, the second mass loss occurred at temperature ranging from 450 to 750°C, where the TG curve displayed a step weight loss (~5.88%) related to the release of structural OH of natural bentonite. The dehydroxylation temperature of ~668°C is in agreement with the classical range of dehydroxylation temperature (600–700°C) observed by other authors for cis-vacant montmorillonites [32].

For the TG and DTG curves of organo-bentonite (shown in Fig. 6), there arised two extra stages, which were ~5.37% from 300 to 450°C and ~2.30% from 450 to 570°C besides the two stages of mass losses corresponding to natural bentonite. This phenomenon was interpreted as an indication that two different types of association took place between the bentonite and the copolymer, which was that the first mass loss was derived from thermal decompostion of the copolymer adsorbed on the surface of bentonite and the second mass loss was assigned to that of the molecules intercalated in the interlayers of bentonite [33]. Moreover, T_{max} (the temperature when the rate of weight loss reaches a maximum) of natural bentonite was observed to be at ~668°C, in contrast, T_{max} of organo-bentonite were 657°C and the intensity of the peak also decreased, which means the dehydroxylation process was induced and the decrement of the interlayer water caused by the intercalation of copolymer molecules, respectively. This was supported by the results obtained from FTIR and XRD studies.

3.4. SEM observation: SEM is a useful technique to study the changes in morphology of bentonite upon modification by surfactants. It is worth to point out that there were not distinct morphologic differences observed between natural bentonite and organo-bentonite, despite the obvious variation observed in the FTIR, XRD and TG analysis. The natural bentonite (Figs. 7*a*–*c*) showed massive aggregated morphology, and there are some large flaky structures. The fragments of small size were relatively regular (Fig. 7*a*). Compared with natural bentonite, there were more particles of smaller sizer and more severely aggregated particles with irregular shapes in organo-bentonite (Fig. 7*d*). Meanwhile, the morphology of flakes transformed to curved plates (Figs. 7*c*, *e* and *f*), which was opposite to the results elsewhere [34]. Hence, the present Letter showed that not only the basal spacing but also the morphology of organo-bentonite strongly depended on the modification of the copolymer (surface adsorption and intercalation).

3.5. HRTEM observation: To find further evidences of the basal spacing enlarging, the microstructure of natural bentonite and organo-bentonite was evaluated by using HRTEM, which permits

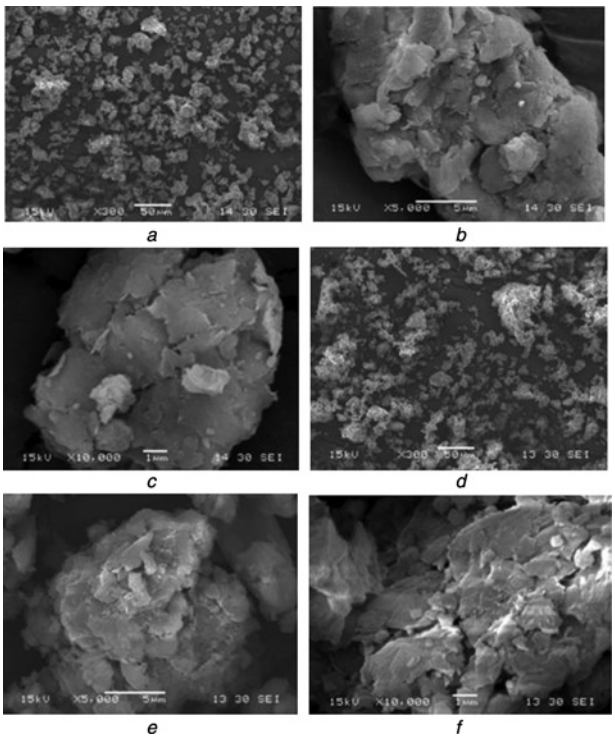

Figure 7 *SEM micrographs*
a–c Natural bentonite
d–f Resultant organo-bentonite

the direct observation of microstructural features of clays. Layers of natural bentonite (Fig. 8*a*) were regular and straight corresponding to the large flakes in the SEM observation. The layer spacing of 1.23 nm was in agreement with the XRD results.

In comparison with natural bentonite, it proved to be difficult to obtain detailed TEM micrographs as the high vacuum of TEM and the high-energy beam can remove the water or surfactant molecules that makes the layer structures collapse and prohibits the structures from being readily observed. Therefore one must take photographs as soon as possible to obtain clear, real images during the period of TEM viewing, especially at high magnifications. In organo-bentonite, irregular intercalated layers can always be observed as shown in Figs. 8*b* and *c* (arrows), which were corresponding to the curved plates in Figs. 7*e* and *f*. However, some regular intercalated layers also occurred (Figs. 8*b–d*). Layer spacings of 1.42 and 1.41 nm were in good agreement with the XRD results, but in some area, the layer spacing remained ~1.24 nm similar to natural bentonite. This indicated that not all the interlayers were intercalated by copolymers, resulting from irregular intercalation or structure collapse mentioned above. Meanwhile, a characteristic swelling of bentonite containing termination as shown by the arrow in Fig. 8*d* also was observed. This suggested that the swelling of silicate layers maybe augmented by defected of the clay structure [35].

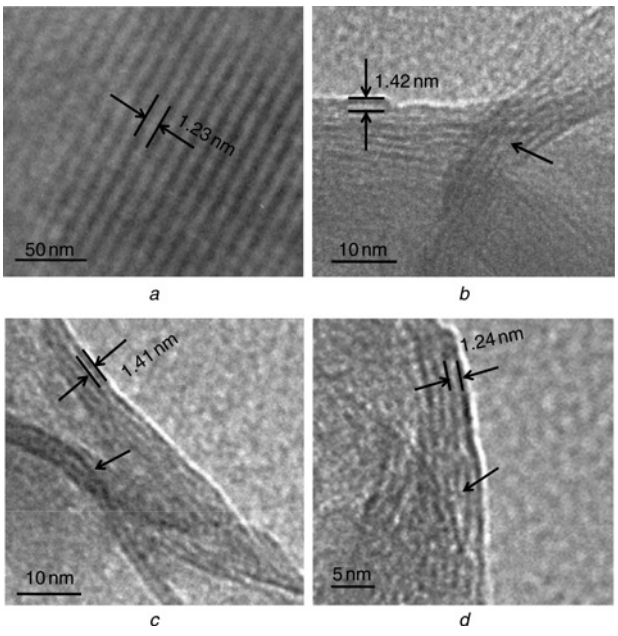

Figure 8 *TEM micrographs*
a Natural bentonite
b–d Organo-bentonite

4. Conclusions: Natural bentonite was successfully modified using polymethacrylate-*g*-PEO comb copolymer. Changes in the surfaces and microstructure of the resultant organo-bentonite were characterised by FTIR, XRD, TG, SEM and HRTEM, respectively.

The two additional peaks at 2923 and 2879 cm^{-1} attributed to the asymmetric and symmetric stretching vibrations of methyl and methylene groups and the decrement of the peak at ~1640 cm^{-1} corresponding to the –OH deformation of water molecules indicated the presence of the copolymer on the surface of organo-bentonite.

Basal spacing enlarging from 1.24 to 1.43 nm showed that the copolymer molecules have been intercalated into the bentonite layers.

Two extra stages of mass losses (~5.37% from 300 to 450°C and ~2.30% from 450 to 570°C) showed thermal decomposition of adsorbed copolymer on the surface and intercalated copolymer in the interlayer of bentonite. T_{max} shift for dehydroxylation temperature (from 668 to 657°C) and the decrement in the density of the peak also supported the occurrence of intercalation process.

More severely aggregated particles with irregular shapes and curved plates in organo-bentonite were observed in comparison with large flaky structures in natural bentonite by SEM viewing.

The TEM micrographs further proved that the interlayers of bentonite were intercalated by copolymers with surface adsorption to a certain extent.

Good agreement was found with the results above and the combined results indicated that modification of polymethacrylate-*g*-PEO comb copolymers was realised through intercalation and surface adsorption rendering bentonite more hydrophobic.

5. Acknowledgments: The financial support (11 nm0501900) from Science and Technology Commission of Shanghai Municipality was gratefully acknowledged. The research was also partially supported by the Science and Technology Cooperation project between Yunnan Province and University/China Academy.

6 References

[1] Karagüzel C., Çetinel T., Boylu F., *ET AL.*: 'Actication of (Na, Ca)-bentonites with soda and MgO their utilization as drilling mud', *Appl. Clay Sci.*, 2010, **48**, pp. 398–404
[2] Mostafa B.A., Assaad F.F., Attia M.: 'Rheological and electrical properties of Egyptian bentonite as a drilling mud', *J. Appl. Polym. Sci.*, 2007, **104**, pp. 1496–1503
[3] Vijayakumar B., Nagendrappa G., Jai Prakash B.S.: 'Acid activated Indian bentonite, and efficient catalyst for esterification of carboxylic acids', *Catal. Lett.*, 2009, **128**, pp. 183–189
[4] Lee W.-F., Chen Y.-C.: 'Effect of bentonite on the physical properties and drug release behavior of poly(AA-co-PEGMEA)/bentonite nanocomposite hydrogels for mucoadhesive', *J. Appl. Polym. Sci.*, 2004, **91**, pp. 2934–2941

doi: 10.1049/mnl.2012.0251

[5] Santiago F., Mucientes A.E., Osorio M., *ET AL.*: 'Preparation of composites and nanocomposites based on bentonite and poly(socium acrylate). Effect of amount of bentonite on the swelling behavior', *Eur. Polym. J.*, 2007, **43**, pp. 1–9
[6] Flores Céspedes F., Villafranca Sánchez M., Pérez García S., *ET AL.*: 'Modifying sorbents in controlled release formulations to prevent herbicides pollution', *Chemosphere*, 2007, **69**, pp. 785–794
[7] Viseras C., Lopez-Galindo A.: 'Pharmaceutical applications of some spanish clays (sepiolite, palygorskite, bentonite): some preformulation studies', *Appl. Clay Sci.*, 1999, **14**, pp. 69–82
[8] Zhou L., Chen H., Jiang X., *ET AL.*: 'Modification of montmorillonite surfaces using a novel class of cationic Gemini surfactants', *J. Colloid Interface Sci.*, 2009, **332**, pp. 16–21
[9] Moreno M., Benavente E., González G., *ET AL.*: 'Functionalizaiotn of bentonite by intercalation of surfactants', *Mol. Cryst. Liq. Cryst.*, 2006, **448**, pp. 123–131
[10] Kollár T., Pálinkó I., Kiricsi I.: 'Effect of heat treatment on amino acid intercalation in montmorillonite', *J. Therm. Anal. Calorimetry*, 2005, **79**, pp. 533–535
[11] Rennig A., Slutter A., Tribe L.: 'Interactions of ammnomethylphosphonic acid and sarcosine with montmorillonite interlayer surfaces', *Int. J. Quantum Chem.*, 2008, **108**, pp. 538–543
[12] Wang T., Zhu J., Zhu R., *ET AL.*: 'Enhancing the sorption capacity of CTMA-bentonite by simultaneous intercalation of cationic polyacrylamide', *J. Hazardous Mater.*, 2010, **178**, pp. 1078–1084
[13] Anirudhan T.S., Ramachandran M.: 'Adsorptive removal of tannin from aqueous solutions by cationic surfactant-modified bentonite clay', *J. Colloid Interface Sci.*, 2006, **299**, pp. 116–124
[14] Tabak A., Baltas N., Afsin B., *ET AL.*: 'Adsorption of reactive red 120 from aqueous solutions by cetylpyridinium-bentonite', *J. Chem. Technol. Biotechnol.*, 2010, **85**, pp. 1199–1207
[15] Shen Y.-H.: 'Preparations of organobentonite using nonionic surfactants', *Chemosphere*, 2001, **44**, pp. 989–995
[16] Safa Özcan A., Erdem B., Özcan A.: 'Adsorption of acid blue 193 from aqueous solutions onto BTMA-bentonite', *Colloids Surf.A, Physicochem. Eng. Aspects*, 2005, **226**, pp. 73–81
[17] Wang L., Wang A.: 'Adsorption properties of Congo Red from aqueous solution onto surfactant-modified montmorillonite', *J. Hazardous Mater.*, 2008, **160**, pp. 173–180
[18] Zohra B., Aicha K., Fatima S., *ET AL.*: 'Adsorption of direct red 2 on bentonite modified by cetyltrimethylammonium bromide', *Chem. Eng. J.*, 2008, **136**, pp. 295–305
[19] Chang J.-H., Jang T.-G., Ihn K.J., *ET AL.*: 'Poly(vinyl alcohol) nanocomposites with different clays: pristine clays and organoclays', *J. Appl. Polym. Sci.*, 2003, **90**, pp. 3208–3214
[20] Huang X., Xu S., Zhong M., *ET AL.*: 'Modification of na-bentonite by polycations for fabrication of amphoteric semi-IPN nanocomposite hydrogels', *Appl. Clay Sci.*, 2009, **42**, pp. 455–459
[21] Plank J., Liu C., Ng S.: 'Interaction between clays and polycarboxylate superplasticizers in cementitious systems', *GDCh-Monographie.*, 2010, **42**, pp. 349–356
[22] Sakai E., Atarashi D., Daimon M.: 'Interaction between superplas-ticizers and clay minerals', *JCA Proc. Cement Concrete*, 2005, **58**, pp. 387–392
[23] Sakai E., Yamada K., Ohta A.: 'Molecular structure and dispersion-adsorption mechanisms of comb-type superplasticizers used in Japan', *J. Adv. Concr. Technol.*, 2003, **1**, pp. 16–25
[24] Cho H.-Y., Suh J.-M.: 'Effects of the synthetic consitions of poly{carboxylate-*g*-(ethylene glycol) methyl ether} on the dispersibility in cement paste', *Cement Concrete Res.*, 2005, **35**, pp. 891–899
[25] Yoshioka K., Sakai E., Daimon M.: 'Role of steric hindrance in the performance of superplasticizers for concrete', *J. Am. Ceram. Soc.*, 1997, **80**, pp. 2667–2671
[26] Lee S.-Y., Cho W.-J., Kim K.-J., *ET AL.*: 'Interaction between cationic surfactants and montmorillonites under nonequilibrium condition', *J. Colloid Interface Sci.*, 2005, **284**, pp. 667–673
[27] Liu B., Wang X., Yang B., *ET AL.*: 'Rapid modification of montmorillonite with novel cationic Gemini surfactants and its afsorption for methyl orange', *Mater. Chem. Phys.*, 2011, **130**, pp. 1220–1226
[28] Eren E., Afsin B.: 'Investigation of a basic adsorption from aqueous solution onto raw and pre-treated bentonite surfaces', *Dyes Pigments*, 2008, **76**, pp. 220–225
[29] Wu Q., Li Z., Hong H., *ET AL.*: 'Adsorption and intercalation of ciprofloxacin on montmorillonite', *Appl. Clay Sci.*, 2010, **50**, pp. 204–211
[30] Frost R.L., Rintoul L.: 'Lattice vibrations of montmorillonite: an FT raman and X-ray diffraction study', *Appl. Clay Sci.*, 1996, **11**, pp. 171–183
[31] Li Y., Ishida H.: 'Concentration-dependent conformation of alkyl tail in the nanoconfined space: Hexadecylamine in the silicate galleries', *Langmuir*, 2003, **19**, pp. 2479–2484
[32] Drits V.A., Besson G., Muller F.: 'An improved model for structural transformations of heat-treated aluminous dioctahedral 2:1 layer silicates', *Clays Clay Miner.*, 1995, **43**, pp. 718–731
[33] Zhou Q., Frost R.L., He H., *ET AL.*: 'Changes in the surfaces of adsorbed *para*-introphenol in HDTMA organoclay – the XRD and TG study', *J. Colloid Interface Sci.*, 2007, **307**, pp. 50–55
[34] He H., Frost R.L., Bostrom T., *ET AL.*: 'Changes in the morphology of organoclays with $HDTMA^+$ surfactant loading', *Appl. Clay Sci.*, 2006, **31**, pp. 262–271
[35] Lee S.Y., Kim S.J.: 'Expansion characteristics of organoclay as a precursor to nanocomposites', *Colloids Surf. A, Physicochem. Eng. Aspects*, 2006, **211**, pp. 19–26